Available online at www.sciencedirect.com

SCIENCE DIRECT®

Biochimica et Biophysica Acta 1556 (2002) 121–132

BIOCHIMICA ET BIOPHYSICA ACTA

BBA

www.bba-direct.com

Transmembrane topology of the NuoL, M and N subunits of NADH:quinone oxidoreductase and their homologues among membrane-bound hydrogenases and bona fide antiporters

Cecilie Mathiesen, Cecilia Hägerhäll*

Department of Biochemistry, Center for Chemistry and Chemical Engineering, Lund University, Box 124, 22100 Lund, Sweden

Received 7 May 2002; accepted 3 September 2002

Abstract

Nicotinamide adenine dinucleotide—reduced form (NADH):quinone oxidoreductase (respiratory Complex I), $F_{420}H_2$ oxidoreductase and complex, membrane-bound NiFe-hydrogenase contain protein subunits homologous to a certain type of bona fide antiporters. In Complex I, these polypeptides (NuoL/ND5, NuoM/ND4, NuoN/ND2) are most likely core components of the proton pumping mechanism, and it is thus important to learn more about their structure and function. In this work, we have determined the transmembrane topology of one such polypeptide, and built a 2D structural model of the protein valid for all the homologous polypeptides. The experimentally determined transmembrane topology was different from that predicted by majority vote hydrophobicity analyses of members of the superfamily. A detailed phylogenetic analysis of a large set of primary sequences shed light on the functional relatedness of these polypeptides.

Keywords: NADH:quinone oxidoreductase; $F_{420}H_2$ oxidoreductase; NiFe-hydrogenase; Antiporter; Fusion protein; Alkaline phosphatase

1. Introduction

Nicotinamide adenine dinucleotide—reduced form (NADH):quinone oxidoreductase or Complex I, is the largest, most complex and least understood of the respiratory chain enzymes. This membrane-bound, multisubunit enzyme catalyzes the oxidation of NADH to NAD^+ and donates electrons to the quinone pool. In this reaction, a flavin mononucleotide and six to eight iron–sulfur clusters serve as intrinsic redox components. In bacteria, Complex I generally contains 14 different subunits, of which 7 are located in the promontory part of the complex, facing the cytoplasm, whereas the remaining polypeptides (NuoA, H, J, K, L, M and N) are very hydrophobic and form the membrane spanning part of the enzyme. The flavin and iron–sulfur clusters are bound to subunits in the promontory part of the enzyme. The electron transfer through the mitochondrial enzyme is coupled to proton translocation across the membrane with a stoichiometry of 4 $H^+/2e^-$ [1]. In addition, the enzyme is capable of $\Delta\mu_H^+$-supported NAD^+ reduction. Although the subject of much speculation, the mechanism of energy transduction is not understood.

The NuoL, NuoM and NuoN subunits (Fig. 1) are homologous protein subunits, which also show sequence similarity to one particular type of antiporter [2]. These polypeptides are most likely important players in the proton translocation machinery of Complex I [3,4], and it is thus extremely important to learn more about their structure and function. In subfractions of mammalian Complex I, the ND5 (NuoL) and ND4 (NuoM) subunits were found close together, but the ND2 (NuoN) subunit was found in another subfraction [5,6]. Most recent low-resolution electron microscopy images of *Escherichia coli* Complex I imply that in one conformational state, the NuoE, F and G subunits of the so-called NADH dehydrogenase module are also in contact with transmembrane antiporter-like subunits [7].

An antiporter of this particular type was first discovered in the alkalophile *Bacillus halodurans* C-125. The gene

Abbreviations: PhoA, alkaline phosphatase; IPTG, isopropyl-thio-β-D-galactoside; NADH, nicotinamide adenine dinucleotide—reduced form; X-phosphate, 5-bromo-4chloro-3-indolyl-phosphate; SDS, Sodium dodecyl sulfate

* Corresponding author. Department of Chemistry and Chemical Engineering, Center for Biochemistry, Lund University, Solvegatan 41 (IDEON gamma-2:G), Lund S-221 00, Sweden. Tel.: +46-46-222-0278; fax: +46-46-222-4534.

E-mail address: Cecilia.Hagerhall@biokem.lu.se (C. Hägerhäll).

0005-2728/02/$ - see front matter © 2002 Elsevier Science B.V. All rights reserved.
PII: S0005-2728(02)00343-2

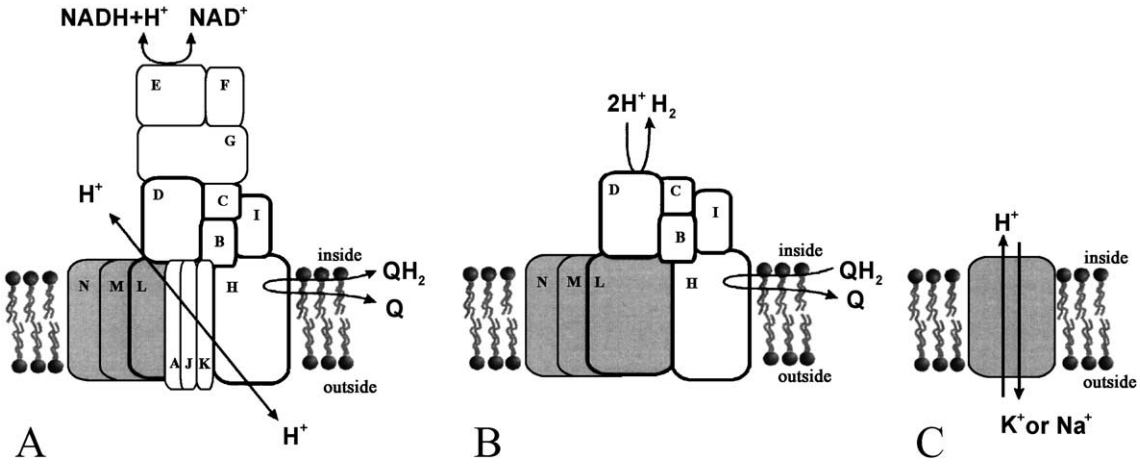

Fig. 1. (A) Schematic outline of respiratory Complex I from bacteria that contains 14 protein subunits (mitochondrial Complex I contains up to 29 additional subunits). The Complex I-like enzymes, NADPH dehydrogenase from chloroplasts and cyanobacteria and the $F_{420}H_2$ oxidoreductase from archea, lack the NuoE, F and G subunits and instead contain different electron input modules. The subunit nomenclature is unfortunately not uniform. The antiporter-like subunits are called NuoL, NuoM, NuoN or NQO12, NQO13, NQO14 in bacterial Complex I, ND5, ND4, ND2 in animal and fungi mitochondria, NAD5, NAD4, NAD2 in plant mitochondria, NdhF, NdhD, NdhB in chloroplasts and cyanobacteria and FpoL, FpoM, FpoN in the archeal enzyme. (B) Schematic outline of membrane-bound, complex NiFe-hydrogenase, which probably can come in variants containing one, two or three antiporter-like polypeptides. However, the actual subunit stoichiometry in the enzyme complexes has not been determined. Note that some NiFe-hydrogenases may function without interaction with quinone or quinone-like substrates [24,54]. The NiFe-hydrogenase module is also outlined in the Complex I enzyme, and Complex I polypeptide names have been used for clarity. Examples of antiporter-like polypeptides in NiFe-hydrogenases are EchA, HycC, CooM, HyfB, HyfD and HyfF. (C) Schematic outline of a bona fide antiporter. It is not known if a single polypeptide forms a functional antiporter, or if multimers are used. Again, the subunit nomenclature is not uniform, and the MrpA-type antiporter can also be called ShaA, YufT, PhaA or MnhA, whereas the MrpD-type antiporter can be referred to as ShaD, YufD, PhaD, or MnhD.

encoding the antiporter was isolated from a mutant, unable to grow at pH 10, demonstrating that this protein was crucial for maintaining neutral cytoplasmic pH under alkaline growth conditions [8]. This type of bona fide antiporter has since been found in many other alkalophile and mesophile bacteria, where it typically appears in a conserved gene context or operon. In *Bacillus subtilis*, the operon contains two different genes, *mrpA* and *mrpD*, encoding polypeptides of this type, together with four genes encoding other, unrelated antiporters and proteins that may play a role for assembly and/or stability of the other polypeptides [9]. A seventh protein encoded by this operon, MrpF, is a Na^+-cholate efflux protein. Both MrpA and MrpD have been shown to have a role in Na^+ resistance and Na^+-dependent pH homeostasis in *B. subtilis* [9–11]. When expressed in *E. coli*, the Mrp antiporter was less active, but more protonophore resistant than NhaA, a classical *E. coli* secondary antiporter [12]. The *mrp* equivalent operon in *Staphylococcus aureus*, named *mnh*, conferred Na^+ resistance when expressed in *E. coli* [13]. In *Rhizobium meliloti*, the MrpA corresponding protein, PhaA, was demonstrated to be a K^+/H^+ antiporter [14]. It remains to be established whether the proteins encoded by the operon form a multisubunit complex or if they function individually in monomeric or multimeric form (see Fig. 1).

In addition, in Complex I and Complex I-like enzymes such as chloroplast NADPH dehydrogenase and archeal $F_{420}H_2$ oxidoreductase, similar antiporter-like subunits are found in the membrane-bound complex NiFe-hydrogenases (hydrogenase-3 and hydrogenase-4) [15]. The physiological function of these hydrogenases is production of H_2, in a non-energy-conserving manner that maintains intracellular pH and redox potential [16]. These hydrogenases are composed of subunits homologous to the Complex I subunits NuoB, C, D, I, and H and can seemingly contain one, two or three antiporter-like proteins (Fig. 1). A plausible evolution of Complex I and Complex I-like enzymes from the membrane-bound complex NiFe-hydrogenases is described by Friedrich and Scheide [17].

In addition, we have found gene clusters containing a gene encoding a homologous antiporter-like polypeptide and a gene encoding a large hydrophilic protein of unknown function in the genomes of *B. subtilis* (accession number BG10949, BG12707), *Vibrio cholerae* (accession number VC1581, VC1582) and *Aquifex aeolicus* (accession number AA0689, AA0690), indicating that a homologous antiporter-like polypeptide might also play a role in a yet unidentified enzyme complex.

There is a small but growing set of studies that indicates that Na^+ or K^+ may be directly involved in the catalytic mechanism of both Complex I [18–20] and the complex, membrane-bound NiFe-hydrogenase [21]. It is thus possible that the antiporter-like subunits in these enzymes are not simply providing means for proton translocation but may still retain a true antiporter function, or the capability to translocate Na^+ or K^+ as well as H^+.

Unfortunately, very little is known regarding the structure and functional mechanism of this type of antiporter, and

even less about the homologous polypeptides in the multisubunit enzyme complexes. In this work, we have experimentally determined the transmembrane topology of the NuoL subunit from *Rhodobacter capsulatus* Complex I using the alkaline phosphatase (PhoA) fusion protein technique developed by Manoil and Beckwith [22], and have constructed a 2D model of the polypeptide that is valid for all these antiporter and antiporter-like proteins. We have also undertaken phylogenetic analyses of the proteins, from which some pertinent indications regarding the function of the polypeptides can be deduced.

2. Materials and methods

2.1. Growth of bacteria

Bacterial strains and plasmids used are listed in Table 1. *E. coli* cells were grown aerobically at 37 °C at 200 rpm in Luria broth medium [23], containing ampicillin (100 μg/ml, Duchefa) when applicable, or kept on Luria broth agar plates (1.5% agar) with the same ampicillin concentration. *R. capsulatus* were grown as *E. coli* but in MPYE medium containing 0.3% peptone, 0.3% yeast extract, 1.6 mM $CaCl_2$ and 1 mM $MgCl_2$. *E. coli* transformants expressing fusion protein were plated on Luria broth agar plates containing ampicillin 100 μg/ml, 5-bromo-4chloro-3-indolyl-phosphate (X-phosphate, Duchefa) 40 μg/ml and isopropyl-thio-β-D-galactoside (IPTG, Saveen) 15 μg/ml.

2.2. Standard molecular biology techniques

Cloning and subcloning was done using standard recombinant DNA procedures as described in Sambrook et al. [23]. Restriction enzymes were from Boehringer Mannheim, Promega or New England BioLabs (NEBL) and dNTPs were from Promega or NEBL. DNA fragments and opened vectors were purified from agarose gel with Jet Sorb Gel extraction Kit (Genomed). DNA ligations were performed at 16 °C overnight or at 4 °C for 60 h using T4 DNA ligase from NEBL or Gibco Invitrogen. *E. coli* cells were transformed by electroporation using a BioRad *E. coli* Pulser™ transformation apparatus and electroporation cuvettes from VWR International. Electrocompetent cells were

Table 1
Bacteria, plasmids and primers used in this work

Bacteria/plasmid	Relevant properties	Reference or source
R. capsulatus ATCC 17015	wild type, (type strain)	DSMZ, Braunschweig, Germany
E. coli XL1-Blue	*recA1*, *endA1*, *gyrA96*, *thi*, *hsdR17*, *supE44*, *relA1* (*lac*)	Promega
E. coli CC118	*araD139 Δ(ara,leu)7697 ΔlacX74 phoAΔ20 galE galK thi rpsE rpoB* $argE_{am}$ *recA1*	[52]
pUC18	amp^R	[53]
pNuoL2	*nuoL*, amp^R	this work
pPHOA	*phoA′*, amp^R	[24]
pNLF1–17	*phoA′*, amp^R	this work
Primers[a]	**Primer sequence**	
SacINuoL	5′-GGA GCT CAA CGT GAT GAA GGG GTA AGG-3′	
NuoLPstI	5′-GGG CTG CAG ATG GAG AGG AGG TTT TGC-3′	
NLF1	5′-CGC CCC CTT TTC CGT GAT CAG C-3′	
NLF2	5′-GAG CGC CCC CGA ACG GAT CC-3′	
NLF3	5′-GGT CAG CCG GTC AAG CCG GAT CC-3′	
NLF4	5′-GAA CCG CGC CTT GTA GGC CTC G-3′	
NLF5	5′-CAG CAG ATA GGA AGC GAC CCC CAC-3′	
NLF6	5′-GCG GTT GAC GAC AAA GGC CTT GAT C-3′	
NLF7	5′-GAG GAA ATGCAG CTC GGT CTT CGC C-3′	
NLF8	5′-GGC GTC GGG CAG CCA GGT GTG-3′	
NLF9	5′-GAC CAT CAT CTT GGC TTC CGG CGC-3′	
NLF10	5′-CGA ATA GGC GAT CAC GCG CTT G-3′	
NLF11	5′-CGC CTT GAA GAA GGC ATG CGT CAG C-3′	
NLF12	5′-CGC CTT GAA GAA GGC ATG CGT CAG C-3′	
NLF13	5′-GGG GAT CTT CTT GCG CAG GCC-3′	
NLF14	5′-GAT GAT CGC GTC TTT CGA GAG ATA GCC-3′	
NLF15	5′-GTC ATG CTT GTG ATG ATC GCC CCG C-3′	
NLF16	5′-GAC ATG GCC CTC GGT CGC GTG TTC-3′	
NLF17	5′-GCC CAG CAC CAT CGC AAA CGC-3′	
Fusseq	5′-TTT TGC AGG TTT ATC GCT A-3′	

[a] Primers were synthesized by the Biomolecular Recourse Facility, Lund University, Sweden, TAG Copenhagen, Denmark and MWG Biotech, Germany.

grown in Luria broth until $A_{600}=0.6-0.7$ and washed twice in 10% glycerol. The final pellet was resuspended in an equal amount of 10% glycerol and frozen in portions of 50 μl at −80 °C. DNA sequencing was performed using Big Dye™ and sequencing by the Sanger method (Applied Biosystems) at the Biomolecular Recourse Facility, Lund University. Small-scale boil preparations of plasmids were done as described in Ref. [23], but using a buffer containing 8% sucrose, 5% Triton X-100, 50 mM Tris–HCl pH 8.0 and 500 μg/ml lysozyme. When cleaner preparations were needed, a phenol extraction step was included [23]. Large-scale plasmid preparations were done using the Jet Star Midi prep kit (Genomed).

2.3. Construction of pNuoL

Chromosomal DNA from *R. capsulatus* ATCC 17015 was prepared as described by Roth and Hägerhäll [24], and included an ethanol precipitation step to increase the DNA concentration. The *nuoL* gene was amplified from the chromosomal DNA by PCR using *Pfu* Polymerase (Stratagene) and the sense primer SacINuoL and antisense primer NuoLPstI (Table 1). The PCR was run as follows: Denaturation 96 °C (3 min), 25 cycles of 96 °C denaturation (45 s), 55 °C annealing (45 s), 72 °C elongation (4 min, 2 min/kbp) and ending with 72 °C (10 min). The resulting DNA fragment containing NuoL and the pUC18 vector was cut with *Sac*I and *Pst*I and the fragment was ligated into shrimp PhoA treated (Boehringer Mannheim) vector. The resulting construct was transformed into *E. coli* XLI Blue by electroporation. Small-scale plasmid preparations from transformants were analyzed by *Bam*HI digestion, that cuts four times in the *nuoL* gene and resulting in fragments of 30, 33, 1794 and 2982 base pairs. Thirty-nine percent of the transformants contained the correct insert. Two clones, named pNuoL1 and pNuoL2, were kept.

2.4. Construction of fusion proteins

PCR amplification of chosen parts of *nuoL* was done using Vent®DNA Polymerase (NEBL) that creates blunt end DNA fragments. PCR reactions were run using pNuoL2 as template, and sense primer SacINuoL and different antisense primers listed in Table 1. Reactions were run with initial denaturation 94 °C (3 min) followed by 25 cycles of 94 °C denaturation (45 s), annealing (45 s, 50–54 °C depending on the primer pair), 72 °C elongation (1 min/kbp). The resulting DNA fragments were digested with *Sac*I, that cuts in the 5′ end of the fragments, before ligation into pPhoA [24] that had been opened with *Sac*I and *Sma*I. The resulting constructs were transformed into *E. coli* CC118 by electroporation. The transformants were analyzed by *Eco*RI digestion of small-scale plasmid preparations or by direct colony PCR. Individual bacterial colonies were picked with sterile toothpicks, re-streaked on plates and the remaining biomass was suspended in 10 μl ddH_2O and boiled for 2 min. Two microliters of the solution was used as template in a 25-μl PCR reaction, identical to the reaction used to create the respective fragment. A strong band of correct size identifies a positive clone. Plasmid was isolated from such clones using the Jet Quick Plasmid miniprep kit (Genomed), and the correct, in frame, gene fusions were confirmed by DNA sequencing using the Fusseq antisense primer (Table 1, Ref. [24]).

2.5. PhoA activity measurements

Liquid cultures were inoculated with fresh bacteria from plates and grown until $A_{600}=0.5-0.7$. Expression of fusion proteins was induced by addition of 1 mM IPTG and growth was continued for 2 h. Cells were permeabilized and assayed according to Manoil [25], using *p*-nitrophenyl phosphate (Sigma Diagnostic) as substrate for PhoA.

$$\text{Units of activity} = \frac{[A_{420} - (1.75 \times A_{550})]1000}{t\ (\text{min}) \times A_{600} \times V\ (\text{ml})} \quad (1)$$

Activity in units was calculated by Eq. (1), where V is the volume of cells, and t is the time during which permeabilized cells are incubated with substrate at 37 °C. A_{600} reflects the cell density in the solution and was measured before substrate addition. A_{550} corresponds to cell debris, and A_{420} monitors the yellow color development of the substrate. A double-beam UV-150-02 spectrophotometer (Shimadzu) or an Ultrospec 4000 UV/Visible spectrophotometer (Amersham Biosciences) was used for the experiment.

2.6. Preparation of membrane vesicles

Membrane protein vesicles for sodium dodecyl sulfate–polyacrylamide gel electrophoresis (SDS-PAGE) and Western blot were prepared from *E. coli* CC118 expressing the different fusion protein constructs, grown and induced as described previously, except that the liquid culture was inoculated with 1% overnight culture. The cells were harvested by centrifugation using a Sorwall SLA 3000 rotor, 15 min at 7000 rpm, washed once in 50 mM KPO_4 buffer, pH 8.0 and stored at −20 °C. Cells were thawed at room temperature and resuspended in 30 mM Tris–HCl pH 7.0, 10 mM KCl and phenylmethansulfonacidfluoride (Sigma-Aldrich) was added to a final concentration of 1 mM. The cell suspension was passed through a French® Pressure cell press (SLM-Aminco, Spectronic instruments) at 6.9×10^6 Pa (1000 psi). Cell debris was removed by centrifugation using a Sorwall SS-34 rotor, 15 min and 8000 rpm, and *E. coli* membranes were obtained by ultracentrifugation of the resulting supernatant using a Beckman 50.2 Ti rotor at 45 000 rpm and 1.5 h. The membranes were resuspended in 30 mM Tris–HCl pH 7.0, 10 mM KCl using a potter, were frozen in liquid N_2 and kept at −80 °C. Protein determination was done with the BCA Protein Assay Kit

(Pierce) with bovine serum albumin (Sigma) as standard and including 1% SDS. The membrane protein preparation was repeated and analyzed twice for each fusion protein construct.

2.7. Western blot

The frozen membrane protein batches were thawed at room temperature, and DNA contamination was removed by treatment with 10 μg/ml DNase (Appligene) for 2 h on ice. SDS-PAGE was done according to Schägger and von Jagow [26] using a stacking gel and 8% separating gel with acrylamide/bis (29:1, BioRad). Samples were boiled for 5 min in loading buffer containing 4% SDS, 12% glycerol, 2% β-mercaptoethanol, 0.1% bromphenol blue, 100 mM Tris–HCl pH 8.8. Electrophoresis was run at 120 V for 11 h using a Protean® II xi electrophoresis unit (BioRad). Rainbow markers RPN 756 (Amersham Biosciences) were used as protein size standard. The gel was washed at room temperature in anode buffer II to remove glycerol. The buffer was exchanged twice during the 5-h incubation on a rocking table.

Proteins were transferred from the gel to Immobilon P membrane filter (Millipore) using a semi-dry blotting apparatus (BioRad) as described in Ref. [27]. Anode buffer II was used as anode buffer and the cathode buffer contained 80 mM 6-amino-*n*-caproicacid. The blot was run at 1.2 mA/cm^2 for 1 h and the filter was subsequently treated in blocking buffer overnight at 4 °C. Detection with antibody was done essentially as described in Ref. [27]. Blocking buffer was 20 mM Tris–HCl pH 7.5, 50 mM NaCl, 0.2% Tween 20 with 5% dry milk. The filter was washed twice in 30 ml blocking buffer without milk, and treated with primary anti-PhoA antibodies (kindly provided by Lars Hederstedt) at 15 000 times dilution for 1 h. Filters were washed as before and treated with PhoA-linked secondary antibody (AKP-linked anti-rabbit Ig from goat, PharMingen, Becton Dickinson) at 12 000 times dilution for 45 min. Finally, filters were washed four times in 30 ml blocking buffer. Filters were developed by incubation with ECF substrate (0.6 mg/ml, Amersham Biosciences) at 6 μg/cm^2 filter. Activities were monitored using a STORM 860 fluorimeter (Molecular Dynamics, Amersham Biosciences) at 650 V. The SDS-PAGE gel was stained with Colloidal Coomassie [28] after blotting to confirm that protein transfer was successful.

2.8. Transmembrane topology prediction methods

The methods used to predict membrane spanning α-helices were HMMTOP [29], TMHMM [30], TopPred2 [31], PHDhtm [32], TMpred [33], DAS [34], SOSUI [35–37] and Kyte and Doolittle [38]. All methods were used with their default values and the single-sequence mode. HMMTOP and TMHMM both use a hidden Markov model formalism in their predictions, TopPred2 creates a standard hydrophobicity plot and then identifies 'certain' and 'putative' transmembrane helices. The TMpred algorithm is based on the statistical analysis of TMbase and a database of naturally occurring transmembrane proteins. The prediction is made using a combination of several weight-matrices for scoring. PHDhtm is based on a neural network predictor. These five methods also predict the orientation of the membrane protein. DAS is based on the dense alignment surface method. The SOSUI prediction is based on the physicochemical properties of amino acid sequences such as hydrophobicity and charges and is developed for finding membrane proteins in whole genome sequences.

2.9. Phylogenic analysis

Multiple alignments of the primary sequences were done with ClustalW [39] using Phylip output format. Default settings were: Slow pairwise alignment, Gonnet series substitution matrix, 10.00 gap opening penalty, 0.20 gap extension penalty, with end gap separation penalty and 8 as gap separation penalty range. Residue specific penalties (Pascarella gaps) that reduce or increase the gap opening penalties at each position in the alignment or sequence were included. Hydrophilic gaps were allowed. Thirty percent delay divergent sequence identities and 0.5 as transition weight (0–1) were used. The PHYLIP package [40] was used with default settings. Phylogenic trees were made by Prodist with a bootstrap before analysis and 100 replicates. Prodist Neighbor computed a consensus tree by analysing the 100 data sets with the Neighbour-Joining method. The distances between the different polypeptides were calculated using Genetics Computer Group software (GCG, Wisconsin Package 10.1, Madison, WI) using distances and no correction. Consensus sequences for the individual phylogenetic clusters (indicated in Fig. 2) were determined with a GCG Pileup of sequences that were run through Pretty. The large data set contained 75 primary sequences chosen to represent all the different enzyme complexes from evolutionary distant organisms: In addition to the polypeptides listed in Fig. 5, we used the sequences of *S. aureus* (MnhA, accession number Q9ZNG6, MnhD Sa, accession number Q9ZNG3), *R. capsulatus* (accession number RRC00609, accession number RRC00612), *Aeropyrum pernix* (SubB, accession number B72619, SubF, accession number F72619, SubA, accession number A72619), *E. coli* (NuoL, accession number P33607, NuoM, accession number P31978, NuoN, accession number P33608), *Thermus thermofilus* (Nqo12, accession number Q56227, Nqo13, accession number Q56228, Nqu14, accession number Q56229), *A. aeolicus* (NuoL, accession number O67340, NuoM, accession number O67341, NuoN, accession number O67342, NuoL, accession number O67389, NuoM, accession number O67390, NuoN, accession number O67391), *Heliobacter pylori* (Nqo12, accession number E71839, Nqo13, accession number F71839, Nqo14, accession number G71839), *Mycobacterium tuberculosis* (NuoL, accession number

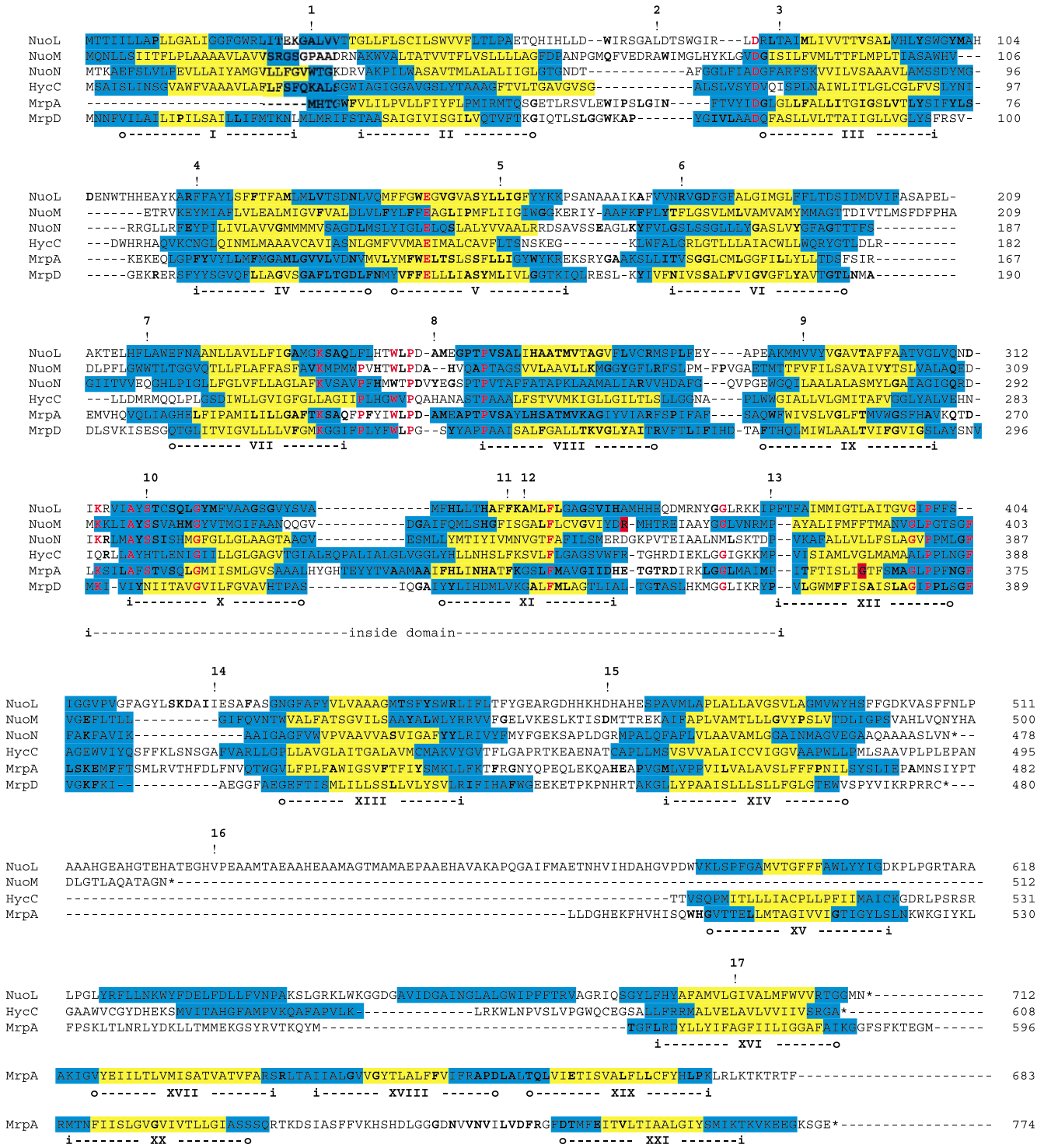

Fig. 2. The primary sequence alignment shows NuoL, M and N from *R. capsulatus* Complex I, HycC from an *E. coli* NiFe-hydrogenase and MrpA and MrpD antiporters from *B. subtilis*. Transmembrane helices predicted with the majority vote approach are indicated below the primary sequences, and consecutively labeled with roman numbers. The stretches of residues where six of eight methods agreed in their prediction of a transmembrane segment are highlighted in yellow, and areas where five or fewer methods agree are marked in blue. The predicted orientation of the transmembrane segments is indicated with i = inside and o = outside and is based on analyses of the MrpD polypeptide only (see text). The location of PhoA fusion points in NuoL is indicated with ! and the corresponding number of the fusion protein. The experimentally determined inside domain between fusion points 10 and 13 is indicated below that predicted. Consensus sequences (>79% identity) are shown in bold letters for NuoL-, NuoM-, NuoN-, MrpA- and MrpD-type polypeptides. The consensus sequence for the entire superfamily is shown in red fonts. Two point mutations discussed in the text are indicated with red box.

O86350, NuoM, accession number O53307, NuoN, accession number O53308), *Nicotina tabacum* chloroplasts (NdhF, accession number P06265, NdhD, accession number P06262, NdhB, accession number P06256), *Synechosystis* sp. strain PCC6803 (accession number sll0026, sll1732, slr2009, sll0027, sll1733, slr1291, slr12007) and *Arabidopsis thaliana* mitochondria (ND5, accession number P29388, ND4, accession number CAA69742, ND2, accession number S71136).

3. Results and discussion

3.1. Predicting the transmembrane topology

The NuoL, NuoM and NuoN polypeptides from *R. capsulatus* Complex I, the HycC polypeptide from an *E. coli* hydrogenase and the bona fide antiporters MrpA and MrpD from *B. subtilis* were used for a detailed analysis, predicting transmembrane helices using the majority vote approach recently described by Nilsson et al. [41]. The polypeptides were individually subjected to eight different methods predicting transmembrane topology (Fig. 2). When six or more of the prediction methods agreed on a stretch of hydrophobic residues, that stretch is shown in yellow, whereas areas predicted as transmembrane by five or fewer methods are marked in blue. As seen in Fig. 2, the antiporters and the different antiporter-like polypeptides generally contain 14 conserved, predicted transmembrane helices. In addition, the NuoL, HycC and MrpA polypeptides contain a C-terminal extension that is not present in the NuoM and N polypeptides or in MrpD. In the N-terminal part, occasional deletions are seen, for instance, the MrpA from *B. subtilis* lacks Helix I (Fig. 2), whereas in ND2/NuoN from *Bovis taurus*, the first three predicted transmembrane segments are absent (not shown). In other MrpA or NuoN polypeptides, these segments are present. Both the N-terminal and the C-terminal domains show little primary sequence similarity compared to the rest of the polypeptide.

Four of the methods, HMMTOP, TMHMM, PHDhtm, and TMpred, were also used in an attempt to predict the orientation of the polypeptides. In the most conserved and central regions, we could get a ‘‘majority vote’’ where three out of four methods agreed in some of the polypeptides but not in others and thus the orientation could not be predicted with confidence. One exception was the MrpD polypeptide, where the four methods produced a unanimous vote. The results from the MrpD prediction are indicated below the primary sequences in Fig. 2.

The overall primary sequence similarity among the different antiporter and antiporter-like polypeptides can be as low as 10%, whereas the hydrophobicity analysis demonstrates that the topology of the different polypeptides nevertheless is conserved. We conclude that the bona fide antiporter polypeptides and the homologous subunits from the complex multisubunit enzymes have a common, conserved structure, in spite of the low absolute primary sequence similarity.

3.2. Experimental determination of the transmembrane topology

To experimentally analyze the transmembrane topology, we used the PhoA fusion protein technique developed by Manoil and Beckwith [22] and the results from the theoretical transmembrane topology prediction in Section 3.1. The NuoL polypeptide from *R. capsulatus* Complex I was used as a model protein. We chose a minimum number of fusion points throughout the polypeptide, as described in Ref. [42]. Fusion points (indicated in Fig. 2) were selected at the end of predicted transmembrane helices, and if present, including positively charged residues that could potentially act as ‘‘stop transfer’’ signals [43]. This method has been successfully applied to a very large number of membrane proteins, summarized in Ref. [42], many of which the topology is either fully or partially confirmed by other methods, cf. Ref. [44].

An expression plasmid, containing the *phoA* gene deleted for the N-terminal signal sequence needed for export of the gene product, was constructed previously [24]. In this plasmid, a recognition site for a restriction enzyme generating blunt ends is used at the upstream end of the truncated gene, to facilitate in-frame insertion of any gene fragment in front of the truncated *phoA*. We subsequently produced *nuoL* fragments of different lengths with PCR using Vent DNA polymerase, that leaves blunt ends. Using this approach, we observed a low frequency of clones containing inserted NuoL fragments of apparently correct size, but containing an extra base pair causing a shift in the following *phoA* reading frame. Such clones could, if the resulting polypeptide was close to the expected size, result in false-negative fusion proteins. Thus, all plasmid constructs were isolated and sequenced over the fusion point (not shown). The fusion proteins were named NLF for NuoL Fusion protein and numbered consecutively 1–17. The fusion proteins were expressed in *E. coli* CC118, a strain from which the *phoA* gene has been deleted. PhoA activity in bacteria expressing fusion protein can be rapidly screened for on IPTG and X-phosphate-containing plates. Subsequently, PhoA activity was assayed directly in permeabilized cells. The results from several independent such experiments are listed in Table 2. To confirm the presence of full-length fusion proteins, isolated membranes from *E. coli* CC118 expressing the fusion proteins were subjected to Western blot analyses using anti-PhoA antibodies (Fig. 3). The constructs are expressed from the lac promotor, leading to production of some amount of protein before IPTG addition. In addition to the full-length fusion proteins, small amounts of proteolytic cleavage products are detected. The PhoA positive constructs, containing a correctly folded PhoA domain (43 kDa), are proteolysis resistant and thus these polypeptides tend to accumulate, whereas the PhoA

Table 2
Alkaline phosphatase activity

Fusion protein	PhoA activity[a] (u)
NLF1	294 ($n=6$)
NLF2	545 ($n=6$)
NLF3	273 ($n=6$)
NLF4	122 ($n=8$)
NLF5	238 ($n=6$)
NLF6	14 ($n=7$)
NLF7	331 ($n=6$)
NLF8	24 ($n=8$)
NLF9	497 ($n=5$)
NLF10	26 ($n=6$)
NLF11	413 ($n=5$)
NLF12	77 ($n=6$)
NLF13	52 ($n=8$)
NLF14	598 ($n=6$)
NLF15	33 ($n=8$)
NLF16	539 ($n=5$)
NLF17	39 ($n=6$)
CC118	2 ($n=2$)

[a] PhoA activity was calculated as in Ref. [25].

negative constructs are more rapidly degraded. It follows that it is not meaningful to attempt to quantify and compare the amounts of fusion protein. In Fig. 3, the total amount of protein loaded in each lane has been adjusted to clearly show the individual full-length fusion proteins.

Expression of the three smallest fusion proteins resulted in cells exhibiting high PhoA activity (Table 2). However, for NLF1, this most likely represents an artifact, since this fusion protein contains only a single transmembrane segment of NuoL. This segment will function as an export signal sequence for PhoA but will not reflect the true transmembrane orientation. NLF2 and 3, which contain positively charged residues before the fusion point, would in case of misfolding rather have ended up on the inside of the membrane; therefore, we believe that these fusion proteins were correctly inserted in the membrane. NLF4 is the first fusion point that we can assign to the inside of the membrane. The NLF5 fusion point is probably located in the middle of Helix V with the result that the PhoA domain is retained on the outside of the membrane. The following fusion proteins give unambiguous results (Table 2). The NLF11 and NLF12 fusion proteins require special mentioning. NLF11 results in a PhoA positive phenotype, whereas NLF12, which contains one additional NuoL amino acid, is clearly PhoA negative. This amino acid is a lysine, conserved in NuoL, which was mistakenly excluded by the Vent polymerase in the isolated NLF11 clone. This illustrates the extreme importance of positively charged amino acids for correct folding and membrane insertion of membrane proteins. The following fusion point, NLF13, is located immediately after the most hydrophilic stretch of amino acids in the polypeptide, and resides on the inside of the membrane. Taking into account the distinct phenotypes of NLF9, NLF10, NLF12, NLF13 and NLF14, we conclude that NLF11 represents a false-positive fusion protein, and that the entire domain containing the predicted transmembrane Helix X and XI is in fact not transmembrane, but is located on the inside of the membrane surface (Fig. 4). Interestingly, this domain also seems to be of functional importance, which will be further discussed in a following section. After the NLF16 fusion point on the outside, the C-terminal domain which is unique for NuoL, begins. One transmembrane segment is followed by a hydrophilic domain residing on the inside of the membrane. The NLF17 fusion protein PhoA domain is retained on the inside, but the fusion point is followed by additional residues that could form a final transmembrane segment (Fig. 4). In addition, a few of the prediction methods we used suggested the presence of two

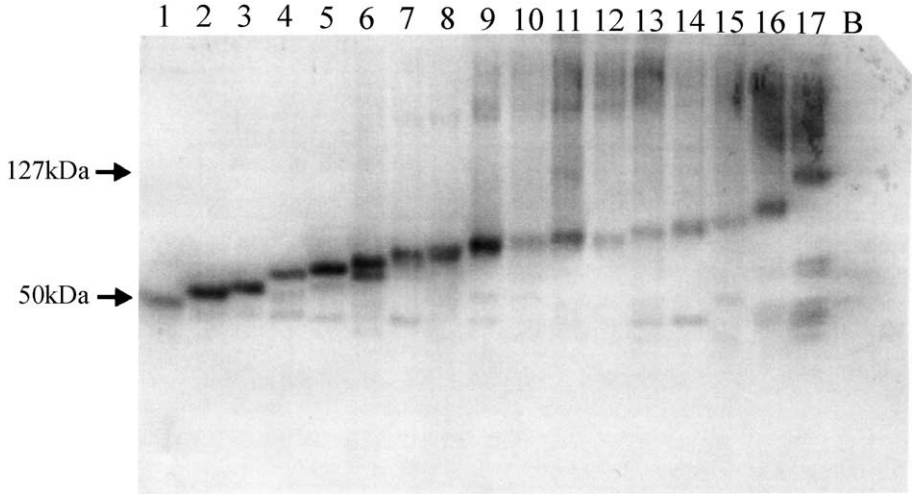

Fig. 3. Western blot of membranes from *E. coli* CC118 expressing fusion proteins NLF1-17. The lanes containing the corresponding fusion proteins are labeled 1–17, the lane labeled B contains plain *E. coli* CC118 membranes. The total amount of protein loaded in each lane was: NLF1, 11 μg; NLF2, 2.6 μg; NLF3, 3.0 μg; NLF4, 5.5 μg; NLF5, 3.6 μg; NLF6, 10 μg; NLF7, 3.8 μg; NLF8, 6.6 μg; NLF9, 3.0 μg; NLF10, 6.1 μg; NLF11, 4.3 μg; NLF12, 4.5 μg; NLF13, 5.7 μg; NLF14, 1.6 μg; NLF15, 13 μg; NLF16, 1.4 μg; NLF17, 8.6 μg and finally for CC118 13 μg.

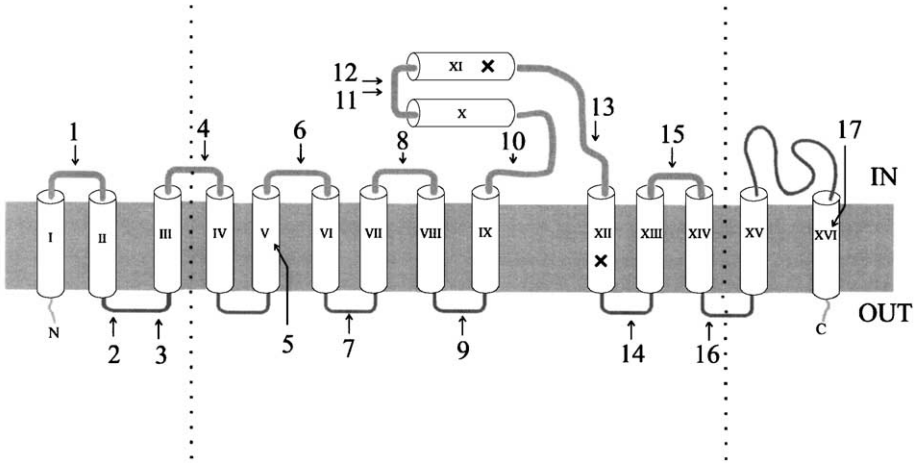

Fig. 4. Transmembrane topology model of NuoL with fusion points indicated. The area between the dotted lines corresponds to the region conserved in all antiporters of MrpA- and MrpD-type and antiporter-like polypeptides of this superfamily. X indicates location of mutations further discussed in the text. Helices are numbered consecutively from the prediction in Fig. 2. The domain between fusion points 10 and 13 most likely rests on the membrane surface, or tilts slightly into the membrane, but is drawn extended for clarity.

additional transmembrane segments between NLF16 and NLF17 (Fig. 2). These have been ignored in the topology model in Fig. 4. It should be noted that the sequence similarity in this domain is very low, even within NuoL polypeptides from different species.

3.3. Phylogenetic analysis shed some light on the function of the polypeptides

The NuoL, M and N subunits of Complex I, the hydrogenase subunits and the bona fide antiporters may have arisen from gene duplication at one or several points during evolution. Thus, the phylogenetic distance relationships of these proteins rather reflect functional differentiation than straightforward evolutionary distance. For a comparison, see Ref. [17], which presents a consensus phylogenetic tree of the NuoB, C, D, H and I subunits from Complex I and the Complex I-like enzymes of chloroplasts and archea and the complex membrane-bound NiFe-hydrogenases, which illustrates the evolutionary relationship of these enzymes.

We have analyzed a large set of polypeptide sequences representing the antiporter-like Complex I polypeptides from mitochondria (8.3% of the sample) and eubacteria of distantly related species (29.2%), from NADPH dehydrogenase from chloroplasts (8.3%) and cyanobacteria (13.9%), and from $F_{420}H_2$ oxidoreductases from archea (12.5%). The set also included polypeptides from complex, membrane-bound NiFe-hydrogenases from both eubacterial and archeal sources and including enzyme variants containing one, two or three antiporter-like subunits (9.7%). It should further be noted that we included only sequences from hydrogenase enzymes that have been biochemically characterized. As bona fide antiporters of MrpA- and MrpD-type we used only those sequences found in the previously described operon context (13.8%). Finally, the three homologous open reading frames (ORFs) of unknown function from *B. subtilis*, *V. cholerae* and *A. aeolicus* were included in the comparison. To access how misalignments in the peripheral parts, where sequence similarity is low, influence the result, we used both the entire sequence, and a subset containing the most conserved region between the fusion points of NLF10 and NLF14. These analyses gave essentially the same result (not shown). A simplified version of the phylogenetic tree, containing a smaller but representative data set using 28 complete primary sequences, is shown in Fig. 5. The analyses show that the NuoL/ND5/NdhF/FpoL, the NuoM/ND4/NdhD/FpoM and the NuoN/ND2/NdhB/FpoN consistently form distinct clusters. Notably, these clusters also include the corresponding archeal and chloroplast subunits, although these latter enzymes are not Complex I. Given the substantial time since the separation of these organisms, such conservation seems to imply that the NuoL, M and N subunits have individual and somewhat different functions within the larger enzyme complex.

The hydrogenase subunits, on the other hand, whether from enzymes containing one, two or three antiporter-like polypeptides, are found randomly scattered in the tree. It thus seems unjustified to label the antiporter-like subunit in membrane-bound, complex NiFe-hydrogenases "NuoL" [16], and to make NuoL part of the "hydrogenase module" and NuoM and N part of the "transporter module" in Complex I [4]. However, the results corroborate the conclusion of Friedrich and Scheide [17] that the last common ancestor of $F_{420}H_2$ oxidoreductase of archea and Complex I of bacteria was a more advanced enzyme than the present-day membrane-bound hydrogenases.

Deletion of either the MrpA or the MrpD antiporter encoding gene from *B. subtilis* resulted in somewhat similar phenotypes under the conditions tested [11]. In our phylogenetic analysis, MrpA and MrpD form individual, distinct

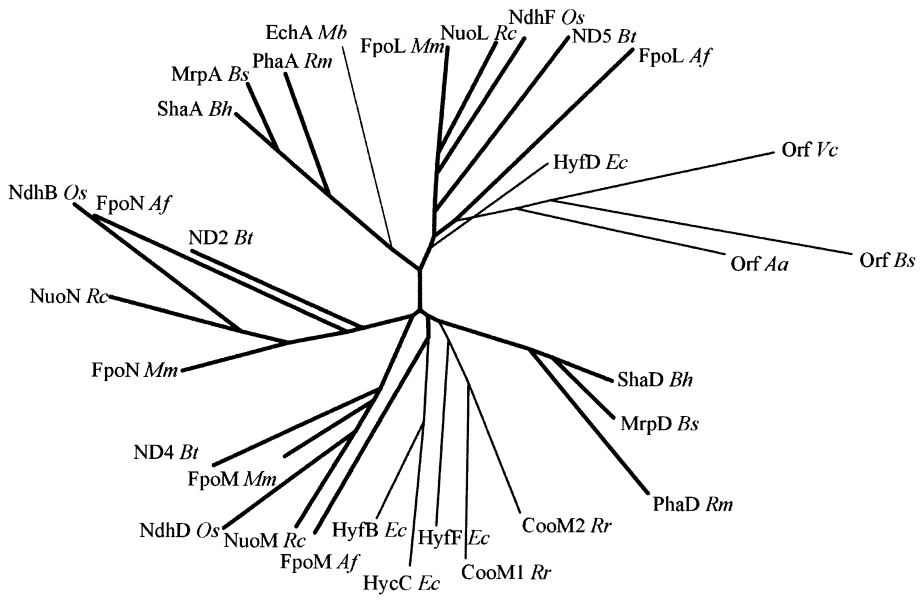

Fig. 5. Unrooted phylogenic tree created by Prodist with bootstrap and 100 replicates. The tree includes: bona fide antiporters from *B. subtilis* (MrpA *Bs*, accession number BG12355, MprD *Bs*, accession number BG12345), *B. halodurans* (ShaA *Bh*, accession number BH1319, ShaD *Bh*, accession number BH1316) and *R. meliloti* (PhaA *Rm*, accession number Q52978, PhaD *Rm*, accession number Q52981); NiFe-hydrogenase subunits from enzymes expressed from operons with one gene encoding an antiporter-like polypeptide *E. coli* (HycC *Ec* accession number P16429) and *Methanosarcina barkeri* (EchA *Mb*, accession number O59652), from an operon containing two antiporter-like equivalents exemplified by *Rhodospirillum rubrum* (CooM *Rr*, accession number U65510) and three antiporter encoding genes as in *E. coli* (HyfB *Ec*, accession number P23482, HyfD *Ec*, accession number P77416, HyfF *Ec*, accession number P77437); $F_{420}H_2$ oxidoreductase subunits from *Archeoglobus fulgidus* (FpoL *Af*, accession number O28449, FpoM *Af*, accession number O28450, FpoN *Af* accession number AF1827) and *Methanosarcina mazei* (FpoL *Mm*, accession number Q9P9F5, FpoM *Mm*, accession number Q9P9F4, FpoN *Mm*, accession number Q9P9F3); NADPH dehydrogenase subunits from *Oryza sativa* chloroplasts (NdhF *Os*, accession number P12129, NdhD *Os*, accession number P12127, NdhB *Os* accession number P12125) and Complex I subunits from *R. capsulatus* (NuoL *Rc*, accession number P50939, NuoM *Rc*, accession number P50974, NuoN *Rc*, accession number P50973) and from *B. taurus* mitochondria (ND5 *Bt*, accession number P03920, ND4 *Bt*, accession number P03910, ND2 *Bt*, accession number P03892). Finally, the ORFs from *B. subtilis* (Orf *Bs*, accession number BG10949), *V. cholerae* (Orf *Vc*, accession number VC1581) and *A. aeolicus* (Orf *Aa*, accession number AA0690) that are found adjacent to a conserved polypeptide of unknown function are included. Simple distance (with no corrections) expressed as observed number of substitutions per 100 amino acids in this data set ranges from 42.58 to 88.22.

clusters in the tree. This, together with the fact that the two polypeptides are often encoded by one operon, indicate that the MrpA and MrpD antiporters may also perform different functions in vivo, and that it could be worthwhile to analyze the properties of these *B. subtilis* deletion strains in greater detail.

It may also be worth noticing that the NuoL-type and MrpA-type polypeptides consistently group closer, and the NuoM-type, NuoN-type and MrpD-type polypeptides form a second group. It is thus possible that both MrpA- and MrpD-type polypeptides were "recruited" to a complex ancestral enzyme, after which a gene duplication of *nuoM* to form *nuoN* or vice versa occurred. An alternative explanation would be convergent evolution. In any case, we can predict that the function of the NuoL-type antiporter-like polypeptide may be more closely related to the function of a MrpA-type antiporter, and that of the NuoM- and NuoN-type polypeptides to the MrpD-type antiporter.

Finally, the antiporter-like ORFs mentioned in the introduction, found in gene clusters in *B. subtilis*, *V. cholerae* and *A. aeolicus* adjacent to a gene encoding a large hydrophilic protein of unknown function, also formed a distinct group in the phylogenetic tree. Deletion of the gene encoding this antiporter-like polypeptide from the chromosome of *B. subtilis* did not result in a pH- or salt-sensitive phenotype (Fröderberg, Mathiesen and Hägerhäll, unpublished data) corroborating that the function of this protein is different from that of MrpA and MrpD. It is likely that this polypeptide is a subunit in an enzyme with yet unknown function.

3.4. Testing the predictive potential of the phylogenetic tree

Synechosystis sp. strain PCC6803 contains a NADPH dehydrogenase similar to that in chloroplasts, composed of 11 subunits corresponding to Complex I subunits, but lacking the NuoE, NuoF and NuoG equivalent subunits [45]. In this organism, the genes are not organized in distinct operons but the sequence of the whole genome has been determined. Most of the NADPH dehydrogenase encoding genes occur in one copy, but there are genes encoding 10 different antiporter-like polypeptides in the genome. These have been assigned as three NdhF (corresponding to NuoL), six NdhD (corresponding to NuoM) and one NdhB (corresponding to NuoN). In a recent study, the six NdhD encoding genes were deleted from the genome, and the properties of the deletion strains were compared. It was

concluded that at least two functionally distinct NADPH dehydrogenases can be made in *Synechosystis*, by varying the composition of antiporter-like polypeptides in the enzyme [46]. We included the 10 primary sequences of antiporter-like polypeptides from *Synechosystis* in our full set of antiporter-like sequences, and repeated the analyses. Three polypeptides (sll0026, sll1732 and slr0844) group with NuoL, one polypeptide (sll0223) groups with NuoN but only four polypeptides (slr0331, slr1291, sll0027 and sll1733) end up in the NuoM cluster. The remaining two polypeptides (slr2007 and slr2009) instead form a subgroup close to antiporters of MrpD type. Interestingly, deletion of these corresponding genes did not result in any significant differences from wild type under the conditions tested, except that the deletion strains grew slower under acidic conditions [46]. We thus suggest that slr2007 and slr2009 are not NADPH dehydrogenase subunits, but rather antiporters of MrpD type.

3.5. Consensus sequences in the transmembrane topology model

We have derived a consensus sequence for all the polypeptides in the family, and consensus sequences for each of the polypeptide subfamilies that form distinct clusters in the phylogenetic tree. The same set of primary sequence was used, except that two additional sequences of antiporters were included. These were *Bacillus firmus* MrpA (AAF21812) and MrpD (AAF21815) and *Deinococcus radiodurans* AAF10453 and G75389. The minimal number of votes required for a consensus was set such that it became as close to 80% identity as possible in each group (NuoL 79%, NuoM 79%, NuoN 79%, MrpA 86%, MrpD 86%). The consensus sequences obtained for each of the groups are marked in bold type in the respective primary sequences in Fig. 2. The group containing the ORFs of unknown function was left out, since only three sequences are available. The residues that are identical in 79% of the entire set of analyzed polypeptides are likewise marked in red in Fig. 2. For the NiFe-hydrogenase subunits, which do not form a phylogenetic cluster, a consensus sequence would correspond roughly to residues marked in red.

The general and the individual consensus sequences can now be related to the common topology model (Fig. 4). Toward the outside of the membrane, we find an aspartate at the beginning of Helix III and a glutamate at the beginning of Helix V in the consensus sequence of all antiporters and antiporter-like polypeptides. A motif toward the end of Helix XII is also conserved. Facing the inside of the membrane, conserved residues are more abundant. Since this consensus sequence describes the full set of sequences including the bona fide antiporters, the bias in similarity toward the inside cannot be related to the interaction with other conserved subunits in the enzymes, which are located on the inside interface of the membrane (Fig. 1). The loop region between Helix VII and VIII contains several generally conserved residues. Amino acid residues in this domain of NuoM in *E. coli* Complex I was recently labeled with an azidoquinone [47] implying the presence of a quinone binding site. The previously discussed large inside domain between Helices IX and XII also contains many residues that are fully conserved (Fig. 2). We attempted to predict the secondary structure of this domain using several algorithms and methods, but obtained very poor agreement between predictions (not shown). In the predicted Helix XI, the consensus sequence motif in the NuoL group and the MrpA group implies the presence of a helical moment, which would result in an amphipathic helix with a conserved face and a hydrophobic face, but there is no such tendency in the other groups. There is no actual sequence similarity between the MrpA antiporter and the K^+ channel [48], but the image of two short helices tipping somewhat into the membrane resembles the structural elements of the ion collector and selectivity filter of the latter protein. As previously mentioned, the functional mechanism of this type of antiporter/antiporter-like polypeptide is unknown on the molecular level. Yet, two amino acid residues located within or adjacent to the inside domain are known to be important for function in the superfamily. In mammalian Complex I, the NuoL, M and N subunits are mitochondrially encoded. The first mutation known to affect function is found in 50% of patients suffering from Leber's hereditary optic neuropathy. In transmitochondrial cybrids carrying the ND4-11778 mutation, the maximal respiratory rate was decreased by 30–36% [49]. The same point mutation (NuoM $R_{368}H$) has been introduced in *R. capsulatus* NuoM to mimic the disease by Lunardi et al. [50]. In *R. capsulatus*, the mutation affected growth under conditions that require a functional Complex I, but had little effect on assays performed with isolated membranes. The second known mutation is a point mutation ($G_{393}R$) in the MrpA-type antiporter that caused an alkali-sensitive phenotype in *B. halodurans* C-125, which led to the first description of an antiporter of this type [8]. The position of these point mutations is indicated with a red square in Fig. 2, and with X in the topology model in Fig. 4.

A recent paper [51] attempts to identify residues responsible for Na^+ translocation by comparing NuoL from *E. coli* and *Klebsiella pneumoniae* Complex I, with MrpA on one hand and NuoL from other Complex I enzymes on the other hand. Unfortunately, few sequences are included in the comparison, and the sequence identity between *E. coli* and *K. pneumoniae*, the only two Complex I known to translocate Na^+, is very high, which hampers the analyses. Tyr139 and Tyr263 are listed as prime candidates for ligating Na^+. As seen in Fig. 2, these residues are not included in the consensus sequence of a larger set of MrpA sequences. Y139 is located in the beginning of Helix V and Y263 in the end of Helix VIII, that is, in the topology model, both residues are located on the outside of the membrane (Fig. 4).

The coupling mechanism of Complex I is unknown, but H^+ pumping was in fact observed in the presence of a specific quinone binding site inhibitor [1]. This may imply

that Complex I is a chimera of a redox-driven and a conformation-driven proton pump [4]. Complex I is capable of both NADH oxidation coupled to H^+ pumping and $\Delta\mu_H^+$-supported NAD^+ reduction, demonstrating that the coupling mechanism must be reversible. At least some, but perhaps all, Complex I are capable of translocating Na^+ [18,19]. In case of the membrane-bound NiFe-hydrogenases, one may speculate that the antiporter-like polypeptide(s) was recruited to provide a transmembrane H^+ channel for H_2 production. An important issue to understand the coupling mechanism is thus whether the antiporter-like polypeptides in the complex enzymes are merely providing channels for one ion species, or if a counter-ion is involved in the reaction. Our topology model and primary sequence analysis of the superfamily of antiporter-like polypeptides provide a basis for addressing these questions.

Acknowledgements

This work was supported by grants from The Swedish Natural Science Research Council, The Crafoord Foundation and from The Hierta-Retzius stipendiefond to C.H. C.M. acknowledges a predoctoral scholarship from The Sven and Lilly Lawski foundation. We thank Prof. Lars Hederstedt for the generous gift of anti-PhoA antibodies.

References

[1] A.S. Galkin, V.G. Grivennikova, A.D. Vinogradov, FEBS Lett. 451 (1999) 157–161.
[2] I.M. Fearnley, J.E. Walker, Biochim. Biophys. Acta 1140 (1992) 105–134.
[3] T. Friedrich, H. Weiss, J. Theor. Biol. 187 (1997) 529–540.
[4] T. Friedrich, J. Bioenerg. Biomembranes 33 (2001) 169–177.
[5] L.A. Sazanov, S.Y. Peak-Chew, I.M. Fearnley, J.E. Walker, Biochemistry 39 (2000) 7229–7235.
[6] L.A. Sazanov, J.E. Walker, J. Mol. Biol. 302 (2000) 455–464.
[7] B. Böttcher, D. Scheide, M. Hesterberg, L. Nagel-Steger, T. Friedrich, J. Biol. Chem. 277 (2002) 17970–17977.
[8] T. Hamamoto, M. Hashimoto, M. Hino, M. Kitada, Y. Seto, T. Kudo, K. Horikoshi, Mol. Microbiol. 14 (1994) 939–946.
[9] M. Ito, A.A. Guffanti, B. Oudega, T.A. Krulwich, J. Bacteriol. 181 (1999) 2394–2402.
[10] S. Kosono, S. Morotomi, M. Kitada, T. Kudo, Biochim. Biophys. Acta 1409 (1999) 171–175.
[11] M. Ito, A.A. Guffanti, W. Wang, T.A. Krulwich, J. Bacteriol. 182 (2000) 5663–5670.
[12] M. Ito, A.A. Guffanti, T.A. Krulwich, FEBS Lett. 496 (2001) 117–120.
[13] T. Hiramatsu, K. Kodama, T. Kuroda, T. Mizushima, T. Tsuchiya, J. Bacteriol. 180 (1998) 6642–6648.
[14] P. Putnoky, A. Kereszt, T. Nakamura, G. Endre, E. Grosskopf, P. Kiss, A. Kondorosi, Mol. Microbiol. 28 (1998) 1091–1101.
[15] M. Finel, Biochim. Biophys. Acta 1364 (1998) 112–121.
[16] L.F. Wu, M.A. Mandrand, FEMS Microbiol. Rev. 10 (1993) 243–269.
[17] T. Friedrich, D. Scheide, FEBS Lett. 479 (2000) 1–5.
[18] W. Krebs, J. Steuber, A.C. Gemperli, P. Dimroth, Mol. Microbiol. 33 (1999) 590–598.
[19] J. Steuber, C. Schmid, M. Rufibach, P. Dimroth, Mol. Microbiol. 35 (2000) 428–434.
[20] K.H. Cho, Y.J. Kim, Mol. Cells 10 (2000) 432–436.
[21] A. Trchounian, K. Bagramyan, A. Poladian, Curr. Microbiol. 35 (1997) 201–206.
[22] C. Manoil, J. Beckwith, Science 233 (1986) 1403–1408.
[23] S. Sambrook, E.F. Fritsch, T. Maniatis, Molecular Cloning. A Laboratory Manual, 2nd ed., Cold Spring Harbor, NY, 1989.
[24] R. Roth, C. Hägerhäll, Biochim. Biophys. Acta 1504 (2001) 352–362.
[25] C. Manoil, Methods Cell Biol. 34 (1991) 61–75.
[26] H. Schägger, G. von Jagow, Anal. Biochem. 166 (1987) 368–379.
[27] L. Ekblad, B. Jergil, Biochim. Biophys. Acta 1531 (2001) 209–221.
[28] V. Neuhoff, N. Arold, D. Taube, W. Ehrhardt, Electrophoresis 9 (1988) 255–262.
[29] G.E. Tusnady, I. Simon, J. Mol. Biol. 283 (1998) 489–506.
[30] E.L. Sonnhammer, G. von Heijne, A. Krogh, Proc. Int. Conf. Intell. Syst. Mol. Biol. 6 (1998) 175–182.
[31] G. von Heijne, J. Mol. Biol. 225 (1992) 487–494.
[32] B. Rost, R. Casadio, P. Fariselli, C. Sander, Protein Sci. 4 (1995) 521–533.
[33] K. Hofmann, W. Stoffel, Biol. Chem. Hoppe-Seyler 347 (1993) 166.
[34] M. Cserzo, E. Wallin, I. Simon, G. von Heijne, A. Elofsson, Protein Eng. 10 (1997) 673–676.
[35] T. Hirokawa, S. Boon-Chieng, S. Mitaku, Bioinformatics 14 (1998) 378–379.
[36] S. Mitaku, M. Ono, T. Hirokawa, S. Boon-Chieng, M. Sonoyama, Biophys. Chem. 82 (1999) 165–171.
[37] S. Mitaku, T. Hirokawa, Protein Eng. 12 (1999) 953–957.
[38] J. Kyte, R.F. Doolittle, J. Mol. Biol. 157 (1982) 105–132.
[39] J.D. Thompson, D.G. Higgins, T.J. Gibson, Nucleic Acids Res. 22 (1994) 4673–4680.
[40] J. Felsenstein, Cladistics 5 (1989) 164–166.
[41] J. Nilsson, B. Persson, G. von Heijne, FEBS Lett. 486 (2000) 267–269.
[42] D. Boyd, in: S.H. White (Ed.), Membrane Protein Structure: Experimental Approaches, Oxford Univ. Press, New York, 1994, pp. 144–163.
[43] G. von Heijne, Y. Gavel, Eur. J. Biochem. 174 (1988) 671–678.
[44] C.H. Yun, S.R. Van Doren, A.R. Crofts, R.B. Gennis, J. Biol. Chem. 266 (1991) 10967–10973.
[45] T. Friedrich, K. Steinmuller, H. Weiss, FEBS Lett. 367 (1995) 107–111.
[46] H. Ohkawa, H.B. Pakrasi, T. Ogawa, J. Biol. Chem. 275 (2000) 31630–31634.
[47] X. Gong, T. Xie, M. Hesterberg, D. Scheide, T. Friedrich, L. Yu, C.-A. Yu, Biophys. J., (2002) 1396 (Pos Board #B451).
[48] D.A. Doyle, J. Morais Cabral, R.A. Pfuetzner, A. Kuo, J.M. Gulbis, S.L. Cohen, B.T. Chait, R. MacKinnon, Science 280 (1998) 69–77.
[49] M.D. Brown, I.A. Trounce, A.S. Jun, J.C. Allen, D.C. Wallace, J. Biol. Chem. 275 (2000) 39831–39836.
[50] J. Lunardi, E. Darrouzet, A. Dupuis, J.P. Issartel, Biochim. Biophys. Acta 1407 (1998) 114–124.
[51] J. Steuber, J. Bioenerg. Biomembranes 33 (2001) 179–186.
[52] C. Manoil, J. Beckwith, Proc. Natl. Acad. Sci. U. S. A. 82 (1985) 8129–8133.
[53] C. Yanisch-Perron, J. Vieira, J. Messing, Gene 33 (1985) 103–119.
[54] J. Meuer, S. Bartoschek, J. Koch, A. Künkel, R. Hedderich, Eur. J. Biochem. 265 (1999) 325–335.